JACS Au
AN OPEN ACCESS JOURNAL OF THE AMERICAN CHEMICAL SOCIETY

pubs.acs.org/jacsau
Article

Poly-Dha Sequences as *Pro*-polypeptides: An Original Mechanistic Postulate Leads to the Discovery of a Long-Acting Vasodilator KU04212

Allen Alonso Haysom-Rodríguez and Steven Bloom*

Cite This: *JACS Au* 2024, 4, 3910−3920
Read Online

ACCESS | Metrics & More | Article Recommendations | Supporting Information

ABSTRACT: The construction of polypeptides was revolutionized by Merrifield's solid-phase synthesis more than half a century ago. Herein, we explore a completely different approach to making peptides. We test an original mechanistic postulate wherein a single peptide made entirely of dehydroalanine (Dha) residues can give rise to regio- and stereodefined peptides by iterative conjugate addition of one- or two-electron nucleophiles. Each nucleophile appends a unique amino acid side chain to the peptide backbone. We show that side chain addition is not random. Side chains are added in one of two ways, in an electrophilicity-gated fashion (most cases) or in a substrate-directed manner, depending on the first nucleophile used in the synthesis. One peptide made in this series, KU04212, a *first-in-class* polyazole peptide, was found to reduce vascular length density (−17%; $p < 0.05$) and increase vessel diameter (124%; $p < 0.001$) in healthy day 6 chick embryos at 24 h post-single dose. It also rescued 75% of the embryos administered a 32-fold lethal dose of ischemia-inducing $CoCl_2$ after 12 h and 12.5% of the embryos after 24 h. In comparison to three mechanistically distinct vasodilators, e.g., isosorbide mononitrate, amlodipine besylate, and prazosin, only KU04212 showed long-acting effects *in vivo*, making it an enticing lead for the treatment of ischemic disorders.

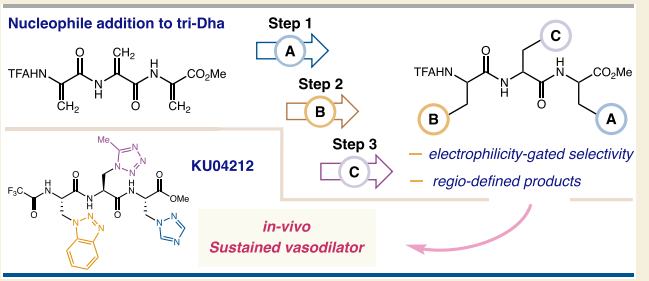

KEYWORDS: *dehydroalanine, pro-peptide, peptide synthesis, electrophilicity-gated, vasodilator, CAM assay*

INTRODUCTION

Solid-phase peptide synthesis (SPPS) is the gold-standard route for making polypeptides. Unfortunately, it is a long and tedious process, requiring one to first make many individual amino acids by traditional *de novo* chemical synthesis, and then to string them together in one precise order using a cocktail of amide bond coupling reagents. Each distinct peptide requires a separate multistep SPPS procedure to complete. To accelerate this process, an entirely new way of making peptides can be envisioned. An ideal platform would allow a single peptide to serve as the progenitor for any number of new peptide sequences, each having any combination of amino acids laced in. One way to do this would be to use a *pro-peptide* consisting entirely of dehydroalanine (Dha) amino acid residues. A Dha residue is a competent Michael acceptor and can intercept one- and two-electron nucleophiles ($\mathbf{R}^{\bullet}$ or $\mathbf{R}:^{-}$), establishing a new amino acid with side chain "**R**" at the former Dha site.[1,2] Over several iterative rounds with different "**R**" donors, one poly-Dha sequence can deliver many polypeptide variants. Not only does this approach enable fully divergent syntheses to be realized, but also eliminates the many protecting group interconversions that plague traditional amino acid preparation and peptide assembly. The innate challenges of this approach are 2-fold: First, how can one control which Dha accepts a new side chain at any point in the peptide synthesis? Second, how can one control the relative stereochemistry of the new side chains as they are introduced? To address these two points, we can treat peptides as innate dipoles. Under physiologic conditions, their *N*-terminus is electron deficient, as the *N*-terminal amine is protonated. The *C*-terminus is electron rich, as the *C*-terminal carboxylic acid is deprotonated. We gathered that this innate phenomenon could be recapitulated on a synthetic poly-Dha sequence by introducing *N*- and *C*-terminal protecting groups with stark differences in their polarities, for instance, a strong electron-withdrawing group (EWG) at the *N*-terminal amine and an electron-donating group (EDG) at the *C*-terminal carboxylic acid, Figure 1. The polarizing effect from these two protecting groups would make each Dha residue electronically distinguishable. Hence, side chain addition could be "*gated*", and therefore, selective, with the

Received: July 6, 2024
Revised: September 15, 2024
Accepted: September 17, 2024
Published: October 7, 2024

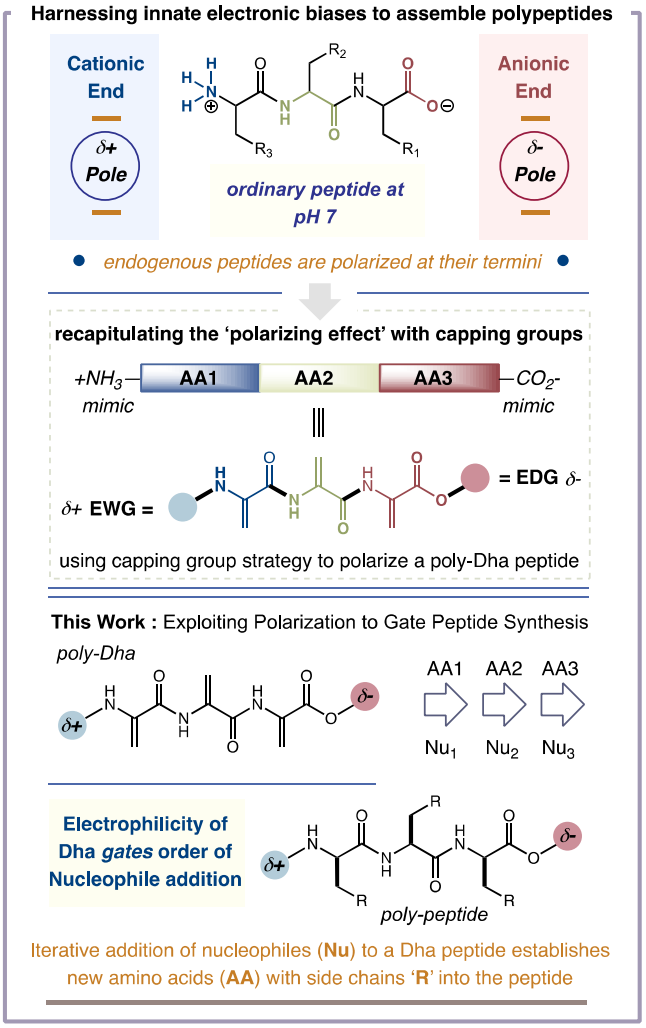

Figure 1. Strategy for constructing synthetic peptides from poly-Dha peptides.

most electrophilic Dha position reacting first and the least electrophilic Dha position reacting last. Regarding stereochemistry, peptides containing consecutive dehydroalanine residues (<6) are completely flat, forming fully extended planar sheets that are stabilized by two types of intramolecular H-bonds, N_i—H---O_i=C′$_i$ —found in 2_5-helical conformations—and $C_{i+1}{}^{\beta}$—H---O_i=C′$_i$, characteristic of all ΔAla peptides. Longer sequences adopt 3_{10}-helical conformations.[3,4] Side chain addition, i.e., the introduction of a new amino acid, disrupts these intramolecular H-bonding networks and implants a new chiral center into the amide backbone of the peptide. Each side chain can then direct the stereochemical delivery of the proceeding side chain addition step, leading to stereospecific outcomes. We now test our mechanistic postulate for building synthetic polypeptides and explore its utility for peptide drug discovery.

RESULTS AND DISCUSSION

Our first challenge was to synthesize a model poly-Dha system. Peptides with more than two consecutive Dha residues are rare, mostly found in natural products, and tend to be isolated from microorganisms.[5,6] Only a few instances of poly-Dha sequences being made by chemical synthesis are reported.[3,7−9] We elected to synthesize a trimer consisting of three covalently linked Dha residues. Peptides with three distinct amino acids, a.k.a. "tripeptides" or "trimers", are very appealing for drug discovery and hit identification due to their cost-effectiveness, possibility for oral administration, and simplicity.[10] They also constitute the minimal structure needed for receptor-specific recognition in living systems,[11] and for the organized assembly of biomaterials.[12,13] But finding which specific sequence is best suited for any one application requires libraries of tripeptides to be evaluated. A tri-Dha template could, therefore, be useful, stamping out a large inventory of chemically distinct tripeptides for testing. Based on precedent from our lab,[14] we tried to assemble the test trimer from a tricysteine peptide. This failed miserably in our hands. The tricysteine peptide afforded a complex mixture of peptide products that included inter- and intramolecular-disulfide cross-links, Dha regioisomers, and peptide-derived polymers. We next examined poly serine peptides. Again, we found no success. Strategies using triasparagine and triaspartic acid peptides were also unsuccessful. Finding no traction with proteinogenic amino acids (Cys, Ser, Asn, Asp),[15,16] we turned to nonproteinogenic residues. While Hoffman elimination of triaminoalanine peptides was ineffective, a peptide containing three (±)-phosphonoglycine residues cleanly converted to the tri-Dha peptide with the combination of aqueous formaldehyde and tetramethylguanidine (TMG) base in THF solvent.[17] This Horner-Wadsworth-Emmons approach worked best when the *N*-terminus of the peptide was capped with a trifluoroacetyl group, and the *C*-terminus was capped with a methyl ester. The tri-Dha peptide TFA-NH-Dha**1**-Dha**2**-Dha**3**-CO_2Me (**1**) was prepared in quantities of up to 500 mg (8.87% overall yield), which is sufficient to test our synthetic concept, Figure 2.

We examined the 1D- and 2D-NMR spectra of **1** and assigned the electrophilicity of each Dha residue. In brief, we first used ^{1}H−^{13}C HMBC and ^{1}H−^{13}C HSQC to determine which ^{13}C signals correlate with the C$^{\beta}$ carbons of each Dha residue. Next, we compared the chemical shifts between these C$^{\beta}$ signals in the ^{13}C spectra of **1**. We determined that *C*-terminal Dha3 was the most downfield signal (most electrophilic site), and internal Dha2 was the most upfield signal (least electrophilic position). *Prima facie*, we would expect nucleophiles (amino acid side chains) to be added to our tripeptide in the order **Dha3** → **Dha1** → **Dha2**, most to least electrophilic. To test this, we first examined a series of thiol nucleophiles, which are well-known to react with Dha residues through conjugate addition.[18] Consistent with our hypothesis, we found that a prototypical thiol, cyclohexanethiol, added primarily to the *C*-terminal Dha3 position of **1**. We isolated this product, **2A**, and examined its 1D- and 2D-NMR spectra. The *N*-terminal Dha1 residue was still more electrophilic then internal Dha2, showing that the relative electrophilicities of the three Dha residues are maintained throughout our synthetic scheme. Subjecting **2A** to a second nucleophile, benzylmercaptan, resulted in a dimodified product **2B**. Addition of the benzyl group occurred selectively at the *N*-terminal Dha1 position. We finished our synthesis by adding a third nucleophile, 2-thioethanol, to the remaining internal Dha2 site, giving a regio-defined tripeptide **2**, as a mixture of *two* major diastereomers (out of *forty-eight* possible regio- and stereoisomers), by ^{1}H NMR, see Supporting Information pg **6**, Table S1, and pg **7**, Table S2, and the ^{1}H NMR presented on pg **54**. The relative stereochemistry of these two major diastereomers was assessed by 2D NOESY NMR. The *C*-

https://doi.org/10.1021/jacsau.4c00603
JACS Au 2024, 4, 3910−3920

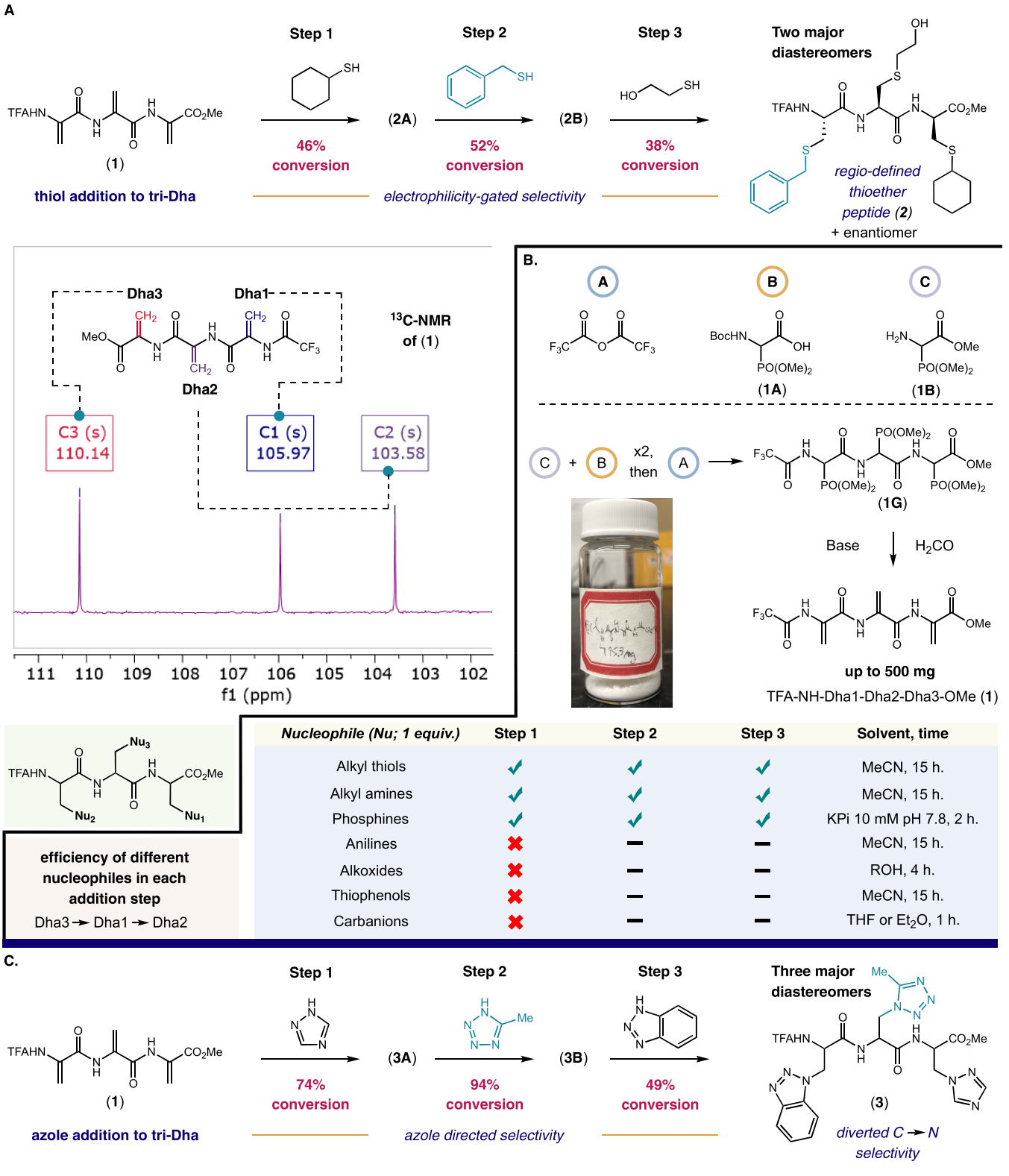

Figure 2. Synthesis and reactivity of (1). (A) Compound **1** follows an electrophilicity-gated reactivity pattern toward conjugate addition with thiol nucleophiles, engaging the most electrophilic dehydroalanine (Dha) position first and the least electrophilic Dha position last. The electrophilic character of each Dha position can be judged by shifts in ^{13}C NMR. (B) Compound **1** can be accessed from commodity chemicals through liquid-phase peptide synthesis. The three Dha residues react in the order Dha3, Dha1, Dha2, with different nucleophiles. (C) Products modified with azole nucleophiles divert the expected order of reactivity, following Dha3, Dha2, Dha1. All conversions were obtained by LC-MS analyses at 214 nm, and are reported as (total % of peptide products after reaction)/(total remaining Dha peptide after reaction) for each step.

https://doi.org/10.1021/jacsau.4c00603
JACS Au 2024, 4, 3910−3920

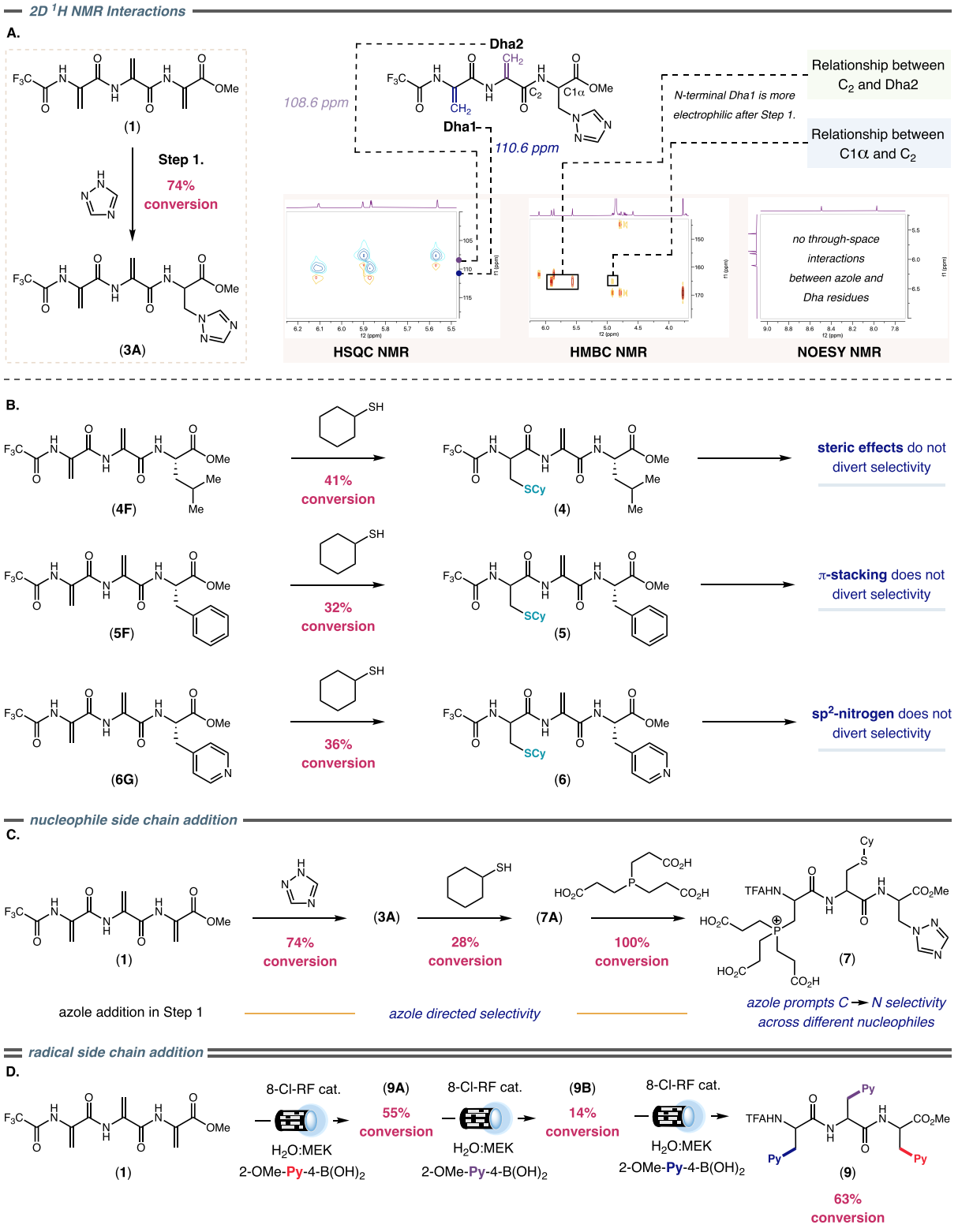

Figure 3. Mechanistic studies. (A) The ^{13}C NMR shifts for Dha carbon atoms do not change after the azole is added to *C*-terminal Dha3, as established by HSQC and HMBC interactions. No interactions between *N*-terminal Dha1 protons and azole protons were detected by NOESY NMR. (B) Electrophilicity-gated pattern is maintained by tripeptides with Leu, Phe and 4-Pyridinyl-alanine residues at the *C*-terminal position, occluding the possibility that steric effects, internal π-stacking, and directing effects from sp^2-nitrogen atoms divert Dha selectivity patterns. (C) The azole ring can direct nonazole nucleophiles to follow a diverted selectivity pattern. (D) The addition of open-shell nucleophiles to (1) follows a diverted selectivity pattern. All conversions were obtained by LC-MS analyses at 214 nm, and are reported as (total % of peptide products after reaction)/(total remaining Dha peptide after reaction) for each step.

https://doi.org/10.1021/jacsau.4c00603
JACS Au 2024, 4, 3910−3920

terminal thiocyclohexane and internal thioethanol side chains are syn, whereas the *C*-terminal thiobenzylic group is anti to both the *N*- and internal-sites, see Supporting Information pg **55**−**58**. One possible explanation for this stereochemical outcome is that addition of benzylmercaptan is guided by steric effects, occurring anti to the cyclohexyl ring. The 2-thioethanol nucleophile prefers to approach from the same side as the smaller cyclohexyl group, as opposed to the larger thiobenzyl group. This same pattern of addition was observed when other alkyl and benzylic thiols were used in random orders. Only thiophenols failed to react. Thus, the addition of three separate nucleophiles is possible, with the site-specificity being gated by innate electronic differences between the Dha residues. This might seem like a rather trivial result, being the expected outcome, but the electrophilicity-gated reactivity of poly-Dha systems has, heretofore, never been demonstrated. Our synthesis presents the first example of this paradigm for building designer polypeptides.

We questioned if other nucleophiles could be used in place of thiols. We found that aliphatic and benzylic amines,[18,19] alkoxides,[20] and trialkylphosphines[21] reacted with **1** over three consecutive steps. Anilines and phenols were not effective. Carbon-based nucleophiles, namely, organometallic reagents, were likewise unsuccessful. The order of Dha reactivity, Dha3 → Dha1 → Dha2, was preserved for each class of successful nucleophile, Figure 2. At this point, we expanded our survey of nucleophiles to include azoles, which have been shown to engage Dha residues through conjugate addition. Some practical advantages of azoles are that they resemble endogenous amino acids but delete at least one hydrogen bond donor, making them useful probes for exploring the importance of specific hydrogen bonds during structure−activity campaigns. Removing hydrogen bonds also makes the peptide more lipophilic, enabling it to better cross cellular membranes.[22] We found that 1,2,4-triazoles and pyrazoles reacted well (30−80% conversion), and at a single Dha site in **1**. When the singly modified products were resubjected to a second panel of azoles, products having two different modifications were obtained (14−94% conversions). The addition of a third azole (49% conversion) delivered a trimodified product. On scale, subjecting 100 mg of **1** to 1,2,4-triazole (a mimetic for histidine[23]) and K_2CO_3 in MeCN solvent[24] afforded a dominant monoaddition product, 74% conversion. Resubjecting the peptide to a second addition step with 5-methyltetrazole gave two major products, 94% conversion (1:2 ratio). Finally, subjecting the two dilabeled peptides to a 1,2,3-benzotriazole nucleophile (a tryptophan mimetic)[25] gave two distinct products, 49% conversion. LC-MS/MS analyses revealed that all *three* major diastereomeric products (out of *forty-eight* possible regio- and stereoisomers) had the same peptide sequence, namely, TFA-NH-(Benzotriazole)-(5-Me-Tetrazole)-(1,2,4-Triazole)-CO_2Me (**3**), which results from the addition order of **Dha3 → Dha2 → Dha1**. This was not the order that we expected, with Dha2 reacting before Dha1, breaking our standard electrophilicity-gated pattern. This diverted pattern of selectivity was maintained with different classes of nucleophiles, so long as azole was used in the first addition step, Figure 2. *But why does this happen?* We considered three possibilities. First, the azole distorts the structure of our peptide such that Dha2 becomes more electrophilic. Second, the azole ring forms an intramolecular π-stacking interaction with *N*-terminal Dha1, shielding it from reaction. Third, the sp^2 nitrogen atoms of the azole ring direct the second nucleophile toward reaction at Dha2, possibly through hydrogen-bonding. We examined each of these scenarios. We synthesized TFA-NH-Dha1-Dha2-(1,2,4-Triazole)-CO_2Me peptide (**3A**) and analyzed its 1D- and 2D-NMR spectra. The *N*-terminal Dha1 position was more electrophilic than Dha2, occluding the possibility of a stereoelectronic change to favor Dha2. We also found no 2D-NMR correlations between the azole ring and Dha1, negating the possibility of a shielding scenario, Figure 3. To test the influence of sp^2 nitrogen atoms, and other factors, we prepared three different peptide sequences, namely, TFA-NH-Dha1-Dha2-**Leu**-CO_2Me (**4F**), TFA-NH-Dha1-Dha2-**Phe**-CO_2Me (**5F**), and TFA-NH-Dha1-Dha2-(**4-Pyr**)-CO_2Me (**6G**). If steric effects cause changes in selectivity, then the Leu residue in **4F** should promote nonelectrophilicity gated selectivity. If π-stacking interactions are at play, then the Phe residue in **5F** should divert selectivity. Finally, if H-bonding through sp^2-nitrogen atoms drives diverted selectivity, then the Pyr moiety in **6G** should cause C → N selectivity. None of these residues diverted the order of Dha reactivity, with all sequences following Dha3 → Dha1 → Dha2, Figure 3. Thus, it appears that *only* azoles divert Dha selectivity, directing nucleophiles to adjoining sites.

We posited that single-electron nucleophiles could react with **1**, following electrophilicity-gated or diverted selectivity patterns. Many catalytic strategies—transition metal, photochemical, electrochemical—are reported to convert Dha residues into new amino acids. The majority of these proceed through carbon-centered radicals ($\mathbf{R}^{\bullet}$) that add to the Dha residue by open-shell conjugate addition. We assessed 20 of these methods (see text in Supporting Information pg **145**−**146** for appropriate references) using 0.42 mg (2.99 μmol) of Ac-NH-Dha-CO_2Me monomer to establish their feasibility on small scale and to probe their competency for applications to our tri-Dha peptide on a 1 mg scale. Of these, *five* conditions yielded the desired conjugate addition product—see Supporting Information pg **10**, Table S6. When applied to our tri-Dha peptide, *three* of these methods gave a monolabeled peptide. Only two of them formed the product in >1% yield. Decomposition of the peptide was the main result in most cases, see Supporting Information pg **11**, Table S7. The two successful methods were a flavin-photoredox chemistry with boronic acids reported by our lab,[14] and a method disclosed by Diao et al. using a nickel/zinc catalytic system and aliphatic halides.[26] Because the latter method is not compatible with aromatic systems, we elected to move forward with our lab's boronic acid chemistry, which is amenable to a wider number of substrates, i.e., aliphatic, aromatic, and heteroaromatic. We optimized our protocol, focusing on photocatalyst identity and the benefit of cosolvents, see Supporting Information, pg **11**−**12**, Tables S8 and S9. Of the thirty-five photocatalysts and twenty-eight solvents surveyed, 8-Cl-Riboflavin (8-Cl-RF) photocatalyst and 10% v:v methyl ethyl ketone (MEK) cosolvent offered modest improvements in yield. We performed our optimized synthetic scheme on a 50 mg scale using 2-(methoxy)pyridinyl-4-boronic acid. When the monolabeled material was resubjected to the same boronic acid, it formed a dimodified product. Reaction of the dimodified peptide with the same boronic acid produced a trimodified product, showing that three separate addition steps is possible. We repeated this exercise to determine the efficiency of each step and deduce the order of Dha reactivity. After each side chain addition step, the labeled material was extracted into

https://doi.org/10.1021/jacsau.4c00603
JACS Au 2024, 4, 3910−3920

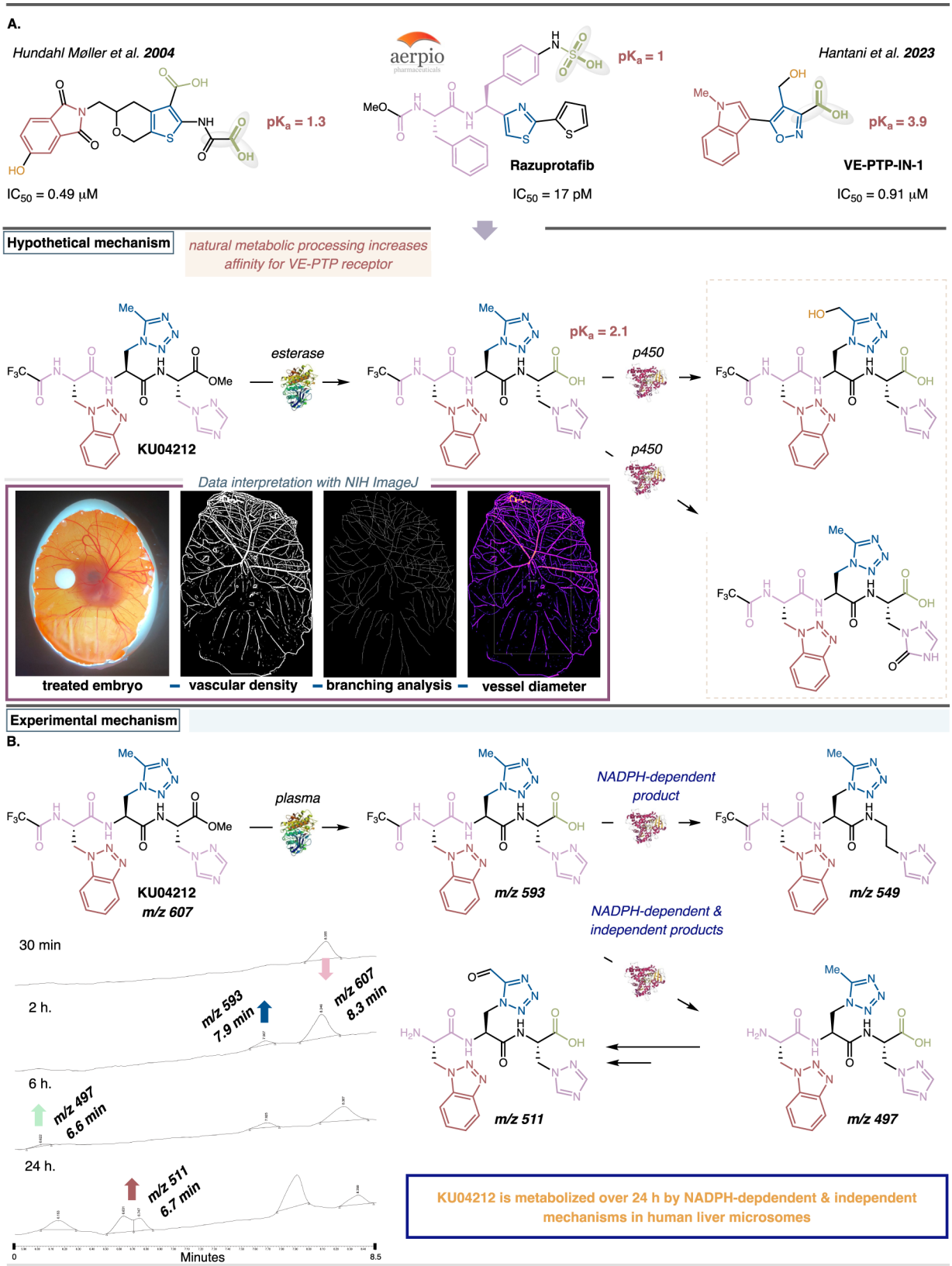

Figure 4. Structural comparison of KU04212 to known drugs and analysis of its metabolic and plasma stability. (A) Known VE-PTP inhibitors have structural similarities to **KU04212** and its predicted metabolites. Their effects on vasculature can be examined using a chick CAM assay and analyzing the results with the NIH ImageJ software package. (**B**) NADPH-dependent and independent metabolites can be detected after incubation of **KU04212** with human liver microsomes. Esterase activity on **KU04212** can be experimentally observed after incubation with human plasma.

ethyl acetate, concentrated, and purified by normal-phase flash chromatography, followed by HPLC. Isolated yields are as follows: Step 1 (5% isolated yield (IY); 46% remaining SM by ^{1}H NMR), Step 2 (23% IY; 16% remaining SM by LC-MS),

https://doi.org/10.1021/jacsau.4c00603
JACS Au 2024, 4, 3910−3920

and Step 3 (9% IY; 0% SM remaining by LC-MS). LC-MS/MS analyses were used to determine the exact sequence of the resulting peptides. In step one, we found ion fragments consistent with a *C*-terminal addition product. For step two, we found ion fragments consistent with the internal and *C*-terminal modified product, leaving the *N*-terminal Dha residue free for reaction in the third step. Thus, we concluded an addition order of **Dha3 → Dha2 → Dha1**, Figure 3. It was extremely difficult to resolve the stereochemistry of our new peptides by 1D- and 2D- ^{1}H NMR and we attempted to generate larger quantities of trimodified product by using different combinations of boronic acids, catalysts, solvents, poly-Dha templates—including an *N*-terminal phthalimide system—, and light sources—see Supporting Information pg **13-14**, Tables S10, S11, and S12. None of these changes improved our overall yield, and, because of limitations in the amount of trimodified product obtained, we were not able to conclude the exact stereochemistry of any peptides made by this route. Regardless, our studies with single-electron nucleophiles (side chain donors) confirms that the order of radical addition is not random and follows *diverted azole selectivity*.

Peptide **3**, and its metabolites, resemble molecules with angiomodulating action at the Tie2/Ang-1 axis, Figure 4.[27−30] Our structures have amide bonds, an indole-like group, five-membered heterocycles, an aliphatic alcohol, and an acidic carboxylic acid. To assess whether **3** could be such a modulator, we performed a chick chorioallantoic membrane (CAM) assay. The CAM is a highly vascularized organ which provides an excellent *in vivo* model for evaluation of compounds with vascular activity.[31] We synthesized TFA-NH-(L)-benzotriazole-(L)-5-Me-tetrazole-(L)-1,2,4-triazole-CO_2Me (**KU04212**),[32] a stereopure variant of our tripeptide, using a liquid-phase route developed by our lab—see text in Supporting Information pg **25−29**—to test in the CAM assay. Regarding stability, we observed that KU04212 maintained its identity and purity in aqueous DMSO solutions for at least three months, as assessed by LC-MS analysis. We thoroughly cleaned and then incubated brown leghorn chicken (*Gallus gallus domesticus*) eggs at 37.8 °C and 50−60% humidity. On day 2, a 1 × 1 cm square opening was carved into the eggshell and the "window" sealed with tape. On day 6,[33] test compounds were separately dissolved in DMSO (40 μM) and 10 μL of the test solution or DMSO vehicle were applied to the CAM on a 6 mm (0.25″) diameter sterile filter disc. On day 7 (24 h post dose), effects on angiogenesis were documented using compound microscopy and the NIH ImageJ software package. We analyzed the number of branching points in the vascular network as a marker of angiogenesis stimulation; vascular density (**VD**) and vascular length density (**VLD**) as markers of neovascularization; and mean vessel diameter as a marker of vasoconstrictive and vasodilative responses. In our first set of experiments, we compared the effects of KU04212 to the known peptidomimetic VE-PTP inhibitor Razuprotafib (AKB-9778). Razuprotafib targets the *intracellular* phosphatase domain of VE-PTP, stabilizing extant vasculature.[34] For this reason, we expected to see pro-angiogenic effects on the CAM after administration of Razuprotafib. Both the anti-Ang1 peptide NH_2−NLLMAAS-CO_2H (**11**) and DMSO vehicle were included as negative controls. Compound **11** competes for the Ang-1 binding site on Tie2, blocking its activity, causing vessel destabilization.[35] We expected to see antiangiogenic effects, i.e., a decrease in branching or vascular density after its administration. We found that **11** (40 mM; n = 2; 1075 mg/kg[36]) had no significant effects on angiogenesis (branching points) and did not affect VD, VLD or vessel diameter, as compared to DMSO control (n = 11), Figures 5 **and** S16; see Supporting Information pg **131**. Razuprotafib (40 μM; n = 5; 0.88 mg/kg) likewise did not affect angiogenesis, VD, VLD or vessel diameter to significant levels when compared with control (n = 11), Figures 5 **and** S16; see Supporting Information pg **131**. (Here we wish to make one comment. When dosed at 40 mM, Razuprotafib was lethal in 7/8 embryos tested. 50% survival (n = 2) was observed at DT_{50} = 400 μM. This effect resembles VE-PTP gene disruption, which is lethal to mice embryos.)[37] KU04212 (n = 10; 40 μM; 0.91 mg/kg), significantly increased vessel diameter (+124%, p < 0.001) and decreased VLD (−17%, p < 0.05) Figure 5. It did not show significant effects on angiogenesis or vascular density when compared to control, Figure S16; see Supporting Information pg **131** (n = 11). When administered at 4 μM (n = 4, 0.09 mg/kg), no significant effects on VLD or vessel diameter were observed, Figure S17; see Supporting Information pg **131**. Vessels at proximal and intermediate distances from the embryo had the most significant increase in diameter, + 114%, p < 0.01 and +110%, p < 0.001, respectively. These include the vitelline arteries and veins. Vessels distal to the embryo, including the chorioallantoic vessels, were not significantly dilated, Figure 6. To document the integrity of the chick vasculature post-treatment, we used a modified version of the well-established Miles Assay, which examines blood vessel permeability. Briefly,

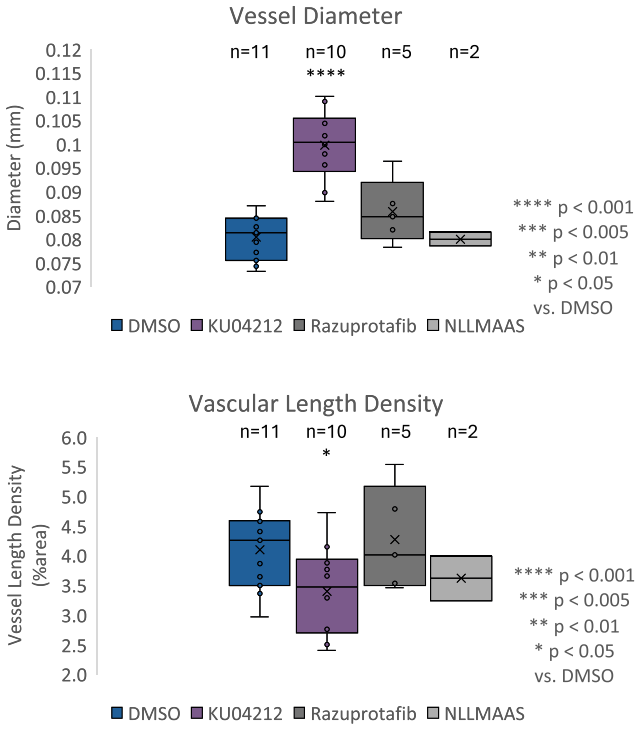

Figure 5. Vasodilatory effects of KU04212. Top: Differences in Vessel Diameter as compared to controls. Bottom: Evaluation of Vascular Length Density as compared to controls. n = number of embryos, boxes represent inner quartiles, error bars indicate variability outside upper and lower quartiles. Data represents average values of all observable CAM area. p-Values were calculated from a two-tailed Student's t test.

https://doi.org/10.1021/jacsau.4c00603
JACS Au 2024, 4, 3910−3920

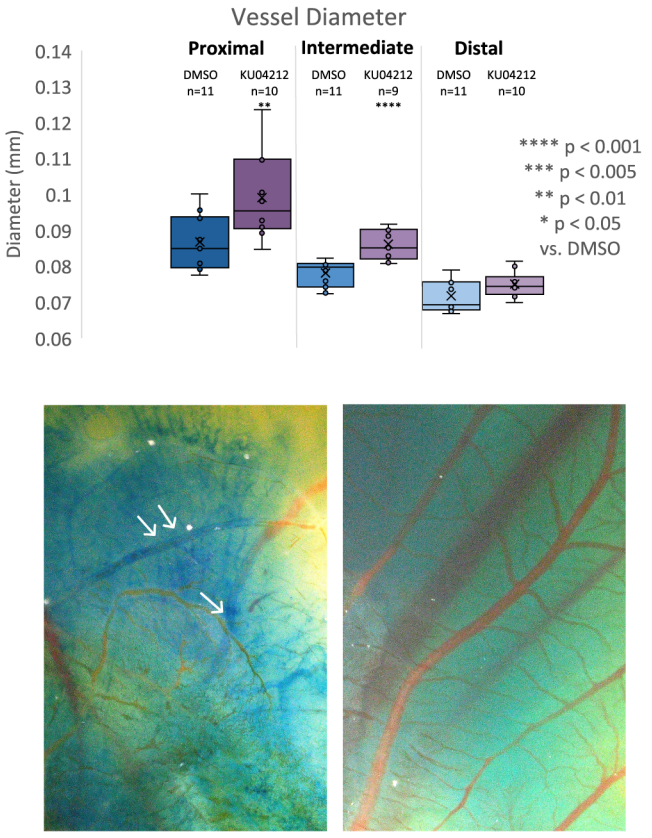

Figure 6. Studies on **KU04212**. Top: Effects of **KU04212** on the average diameter of vessels that are proximal (left), at an intermediate distance (center) and distal (right) to the embryo in comparison to DMSO control. Bottom: Miles assay; left photo depicts the CAM of an embryo treated with compound **11**, and the right photo shows the CAM of an embryo treated with **KU04212**. Notice Evan's blue infiltration into vessels (white arrows) after treatment with compound **11**, as opposed to when treated with **KU04212**. *n* = number of embryos, boxes represent inner quartiles, error bars indicate variability outside upper and lower quartiles. p-Values were calculated from a two-tailed Student's *t* test.

Evans Blue dye is injected into the yolk sac of the treated egg. The dye leeches into more permeable, often malformed, vessels, staining them blue. After 30 min, the CAM is fixed with 1:1 Acetone/MeOH, washed with saline to remove excess dye, and analyzed by compound microscopy. No dye uptake was evident after treatment with KU04212 or DMSO control. Conversely, after treatment with compound **11** control, dye uptake was clearly visible, Figure 6. This shows that KU04212 does not compromise vessel structure. We finally performed a time study to document the effects of KU04212 (40 μM, 0.91 mg/kg) at 1-, 6-, 12-, 24-, and 48-h post administration, as compared to control embryos. We observed a modest, but significant ($p < 0.05$), increase in vessel diameter after 1 h. An increase was also observed after 6 h of administration, but the vessel diameter was not significantly different than control. Vessel diameters between control and treated embryos were nearly identical at 12 h, followed by a dramatic increase in vessel size in the treated embryos at 24 h. This significant increase disappeared by 48 h, Figure S18; see Supporting Information pg **132**.

One way to interpret the above results is that KU04212 displays some vasodilatory activity in the first few hours after administration. The parent compound is a mild vasodilator. After a few hours, KU04212 is biotransformed into a more active metabolite that reaches a peak activity around 24 h. Its effect then recedes over the next 24 h, losing activity by 48 h. We studied the proclivity for such a pathway using human plasma and human liver microsomes at high-equivalent concentrations of KU04212 (1 mM; a 100- to 1000-fold greater concentration of drug than traditional experiments), Figure 4. In human plasma, KU04212 was rapidly converted to the corresponding free *C*-terminal carboxylic acid; ∼ 87% conversion after 2 h; see the LC spectrum in Supporting Information pg **136**. In contrast, the control drugs, verapamil and losartan, were not metabolized in plasma after 2 h. In human liver microsomes, we found that KU04212 was metabolized through NADPH-dependent and -independent mechanisms, producing a series of time-dependent metabolites. Without NADPH, we observed: (1) free *C*-terminal acid, (2) free *N*-terminal amine and *C*-terminal acid, and (3) a sequence having a carbonyl group incorporated within the completely unprotected peptide. This final oxidized metabolite was only formed in small amounts, and we were not able to confirm its structure. However, based on ion fragments detected by LC-MS/MS (see MS and MS/MS spectra in Supporting Information pg **139**), we surmise that its identity is likely an aldehyde, formed by oxidation of the methyl group on the central tetrazole ring of KU04212. The only observed NADPH-dependent metabolite was a *C*-terminal decarboxylated version of KU04212, Figure 4. Taken together, our pharmacokinetic (plasma + microsomal) studies support a mechanism in which KU04212 is rapidly converted to the free *C*-terminal carboxylic acid in plasma and then metabolized by a series of NADPH-independent and -dependent enzymes to produce at least three additional metabolites, namely, a fully unprotected peptide at *N*- and *C*-termini, a carbonylated product, and a decarboxylated analog. This sequence of events tracks well with the activity time-course of KU04212 in chicks, exhibiting modest activity in the first few hours followed by a considerable spike in activity around 12 h, which can be consistent with the formation of more active metabolites.

An increase in vessel diameter can be a consequence of Tie2/Ang-1 pathway activation, which can happen through three different mechanisms: (1) overexpression of Ang1, which increases $NO^{\bullet}$ production by endothelial nitric oxide synthase (eNOS), (2) targeting of the *extracellular* fibronectin type III-like repeat domain of VE-PTP, leading to receptor endocytosis and ERK1/2 signaling, or (3) migration of endothelial cells (hyperplasia) into developing vessels by high concentrations of VEGF.[38] If KU04212 operates through the first mechanism, administration of Ang-1 should be able to recapitulate its effects; if it operates through the second mechanism, antibody-specific engagement of the extracellular fibronectin type III-like repeat domain of VE-PTP should be able to recapitulate its effects; and if it operates through the third mechanism, then administration of VEGF should be able to recapitulate its effects. To test these scenarios, we used human Ang-1 protein (Gibco, 18.87 μM, $n = 2$; 0.75 mg/kg), Ms monoclonal antibody to VE-PTP [122.2] (Abcam, 1 mg/mL, $n = 2$; 0.75 mg/kg), and recombinant human VEGF 165 protein (Gibco 18.87 μM, $n = 3$; 0.75 mg/kg). None of these agents gave results consistent with KU04212 (Figure S19, see Supporting Information pg **132**), suggesting that it does not affect the Tie2/Ang1 axis and elicits its biological effect through a different mechanism of action.

https://doi.org/10.1021/jacsau.4c00603
JACS Au 2024, 4, 3910−3920

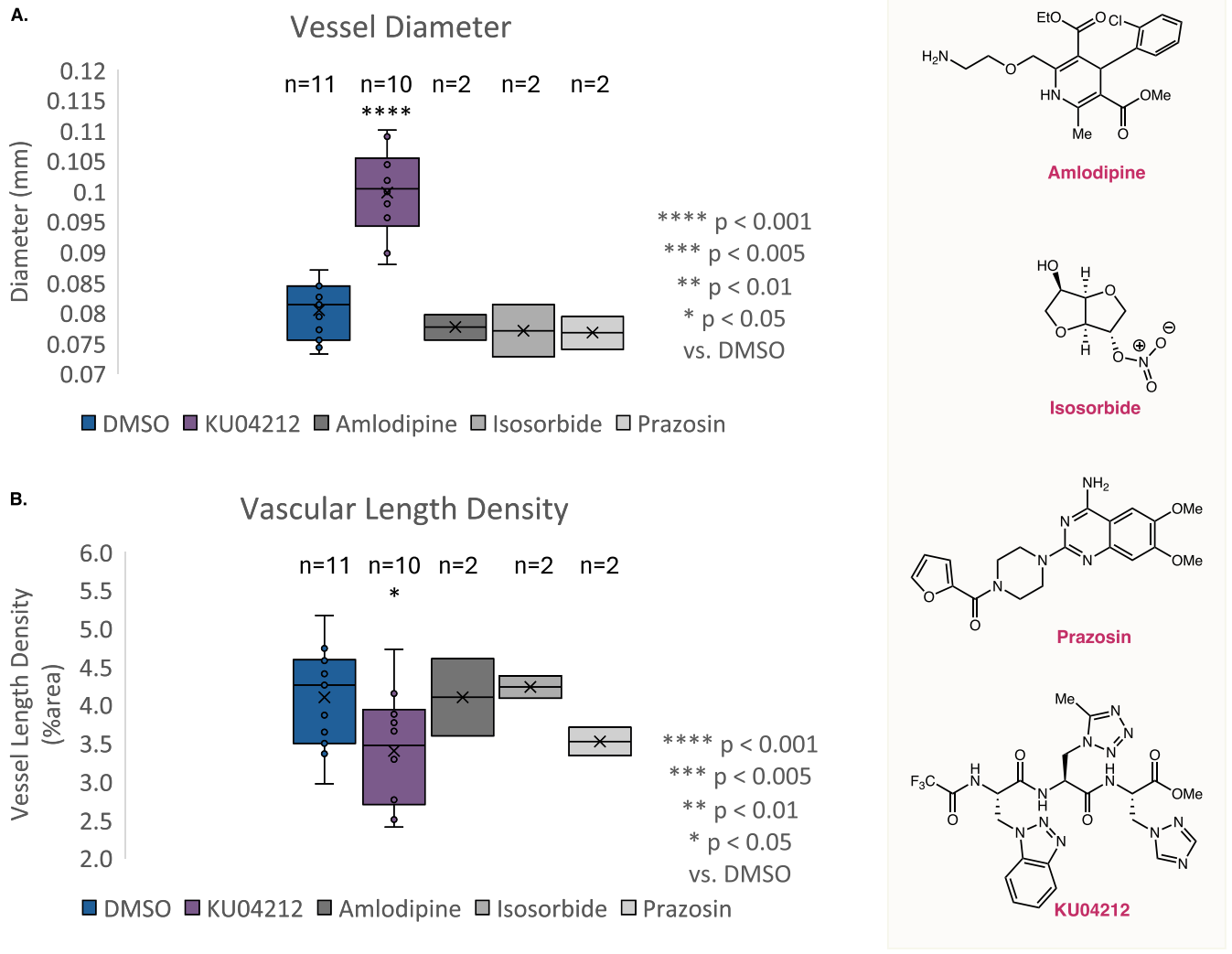

Figure 7. Comparison of the effects of KU04212 with those of known vasodilators. (A) Comparison of the effects in Vessel Diameter. (B) Comparison of the effects in Vascular Length Density. Structures of evaluated compounds on the right. DMSO and KU04212 data is the same as presented in Figure 5. n = number of embryos, boxes represent inner quartiles, error bars indicate variability outside upper and lower quartiles. p-Values were calculated from a two-tailed Student's t test.

To explore alternative mechanisms, we assessed five mechanistically distinct vasodilators. Perhaps one of these would parallel the results obtained with KU04212. Some of the most common vasodilatory drugs include nitric oxide (NO) donors, calcium channel blockers—particularly dihydropyridines, which act on L-type calcium channels in vascular smooth muscle without significant action on the heart—, adrenergic antagonists—especially α_1-adrenergic antagonists, since α_1-adrenergic receptors are expressed in vascular smooth muscle—, and inhibitors of the renin-angiotensin pathway, namely, angiotensin converting enzyme inhibitors (ACEI) and angiotensin II receptor blockers (ARB). In the clinic, these substances are used to treat cardiovascular diseases, such as angina pectoris.[39] We tested isosorbide mononitrate (an NO donor), amlodipine besylate (a dihydropyridine calcium channel blocker), losartan hydrochloride (an ARB), and prazosin (an α_1-adrenergic antagonist). We also included bradykinin in this analysis since it is a strong endogenous vasodilator peptide. All compounds, excluding bradykinin, were dosed at 40 μM for direct comparison to our azole tripeptide. We found that bradykinin (18.87 μM, n = 3, 0.75 mg/kg) and losartan (40 μM, n = 3, 0.632 mg/kg) were lethal. No embryos survived after 24 h following losartan administration and only one embryo survived after 24 h of bradykinin administration. Vessel rupture was observed in both cases, and we did not perform statistical analyses on these runs. 67% of the embryos treated with amlodipine (40 μM, n = 3, 0.611 mg/kg) or isosorbide (40 μM, n = 3, 0.286 mg/kg) survived, and 100% of the embryos treated with prazosin (40 μM, n = 2, 0.573 mg/kg) survived. However, none of these compounds produced any significant effects on VLD or vessel diameter at 24 h post-single dose; although it has been shown that these agents do dilate chick embryo vessels in less than 1 h.[40] Only KU04212 produced the desired phenotype at 24 h, Figure 7.

Because KU04212 has both early (at 1 h) and late (at 24 h) vasodilator activity, it might have significant effects in a disease model of ischemia. Treating the CAM with $CoCl_2$ induces severe ischemia and teratogenic effects. We coadministered a 32-fold lethal dose (32× LD_{50})[41] of $CoCl_2$ hexahydrate (1.2 mg, 0.54 M) with KU04212 on the CAM of Day 6 embryos. Effects were determined 12- and 24-h post-single dose. Embryos treated only with $CoCl_2$ showed 100% mortality

https://doi.org/10.1021/jacsau.4c00603
JACS Au 2024, 4, 3910−3920

after 12 h (n = 4) and 24 h (n = 8). 75% of embryos treated with both KU04212 and $CoCl_2$ survived after 12 h (n = 4), and 12.5% after 24 h (n = 8). We considered the possibility that this result could be explained by cobalt chelation to the azole side chains of KU04212, preventing it from inducing toxic effects. However, this is extremely unlikely as we are administering 13,500 mol equiv of cobalt relative to KU04212. Hence, KU04212 may offer some benefits in toxic dose settings, a result that could be very consequential for treating many ischemic disorders. For example, the CAM is comparable to the epithelial layer surrounding the coronary arteries of the human heart. Vessels contained in the CAM, particularly the vitelline arteries, respond to drugs (vaso-constrictors and vasodilators) and atherosclerotic plaque and its' drivers—cholesterol, age, Ca^{2+}, lipoprotein—in a similar way to coronary arteries.[42−46] Abnormal vasculogenesis/angiogenesis on the CAM also causes the embryo to display a pattern of cardiac failure that is similar to humans in end-stage heart failure. The CAM can, therefore, model coronary heart disease. Lethal doses of $CoCl_2$ represent chronic coronary occlusion and myocardial infarction. Having 75% of embryos survive *extreme* doses of $CoCl_2$ for 12 h, and 12.5% for 24 h, means that KU04212 not only staves off myocardial toxicity but promotes long-term survival. These important findings constitute the premise of our future work which aims to study KU04212 in higher order mammals, including those with coronary heart disease.

CONCLUSIONS

In summary, we show that poly-Dha sequences can give rise to polypeptides through the regio- and stereocontrolled addition of one- and two-electron nucleophiles. This discovery demonstrates that an entirely new way of building peptides is indeed possible. By using azoles as side chain donors, we identified a peptide, KU04212, with long-acting vasodilatory effects *in vivo* that also extends survival rates in an ischemia model. Future efforts will focus on improving our approach, determining the pharmacological impact of observed metabolites, and studying the therapeutic potential of KU04212 in higher-order mammals, especially in cardio-toxic and -disease models.

MATERIALS AND METHODS

All experimental procedures and compound information is included in the SI Appendix. No unexpected or unusually high safety hazards were encountered.

ASSOCIATED CONTENT

Supporting Information

The Supporting Information is available free of charge at https://pubs.acs.org/doi/10.1021/jacsau.4c00603.

Material information, procedures, data tables, compound characterizations, examples of calculations and pharmacokinetic data (PDF)

AUTHOR INFORMATION

Corresponding Author

Steven Bloom − *Department of Medicinal Chemistry, University of Kansas, Lawrence, Kansas 66045, United States;* orcid.org/0000-0002-4205-4459; Email: spbloom@ku.edu

Author

Allen Alonso Haysom-Rodríguez − *Department of Medicinal Chemistry, University of Kansas, Lawrence, Kansas 66045, United States;* orcid.org/0000-0002-6990-9648

Complete contact information is available at: https://pubs.acs.org/10.1021/jacsau.4c00603

Notes

The authors declare the following competing financial interest(s): The authors have filed a United States Provisional Patent on KU04212 (patent number: 63/639,361.

ACKNOWLEDGMENTS

This work was performed in the Department of Medicinal Chemistry at the University of Kansas, and supported by the School of Pharmacy, University of Kansas, and the National Institute of General Medical Sciences (NIGMS) of the National Institutes of Health under Grant R35GM147169. The content is solely the responsibility of the authors and does not necessarily represent the official views of the National Institutes of Health. The authors thank Samuel Gary, Pei-Hsuan Chen and Farjana Afroj of the University of Kansas for their help in reviewing the manuscript.

REFERENCES

(1) Bogart, J. W.; A A Bowers, A. A. Dehydroamino acids: chemical multi-tools for late-stage diversification. *Org. Biomol. Chem.* **2019**, *17*, 3653−3669.

(2) Peng, X.; Xu, K.; Zhang, Q.; Liu, L.; Tan, J. Dehydroalanine modification sees the light: a photochemical conjugate addition strategy. *Trends Chem.* **2022**, *4*, 643−657.

(3) Crisma, M.; Formaggio, F.; Toniolo, C.; Yoshikawa, T.; Wakamiya, T. Flat peptides. *J. Am. Chem. Soc.* **1999**, *121*, 3272−3278.

(4) Benavides, I.; et al. Poly(dehydroalanine): Synthesis, properties, and functional diversification of a fluorescent peptide. *J. Am. Chem. Soc.* **2022**, *144*, 4214−4223.

(5) Fate, G. D.; Benner, C. P.; Grode, S. H.; Gilbertson, T. J. The biosynthesis of sulfomycin elucidated by isotopic labeling studies. *J. Am. Chem. Soc.* **1996**, *118*, 11363−11368.

(6) Murphy, A. C.; Corney, M.; Monson, R. E.; et al. Biosynthesis of antifungal solanimycin may involve an iterative nonribosomal peptide synthetase module. *ACS Chem. Biol.* **2023**, *18*, 1148−1157.

(7) Biondi, B.; et al. Flat, ferrocenyl-conjugated peptides: A combined electrochemical and spectroscopy study. *ChemElectroChem* **2021**, *8*, 2693−2700.

(8) Santi, S.; Bisello, A.; Cardena, R.; et al. Flat, $C^{\alpha,\beta}$-didehydroalanine foldamers with ferrocene pendants: assessing the role of α-peptide dipolar moments. *ChemPlusChem* **2021**, *86*, 723−773.

(9) Rangachari, V.; Davey, Z. S.; Healy, B.; et al. Rationally designed dehydroalanine (ΔAla)-containing peptides inhibit amyloid-β (Aβ) peptide aggregation. *Biopolymers.* **2009**, *91*, 456−465.

(10) Santos, S.; Torcato, I.; Castanho, M. A. R. B. Biomedical applications of dipeptides and tripeptides. *Biopolymers* **2012**, *98*, 288−293.

(11) Ung, P.; Winkler, D. A. Tripeptide motifs in biology: targets for peptidomimetic design. *J. Med. Chem.* **2011**, *54*, 1111−1125.

(12) Brito, A.; Dhwanit, D.; Lampel, A.; Castro, I. V. I. B.; Kroiss, D.; Reis, R. L.; Tuttle, T.; R V Ulijin, R. V.; Pires, R. A.; Pashkuleva, I. Expanding the Conformational Landscape of Minimalistic Tripeptides by Their O-Glycosylation. *J. Am. Chem. Soc.* **2021**, *143*, 19703−19710.

(13) Kulkarni, K.; Kelderman, J.; Coleman, H.; Aguilar, M. I.; Parkington, H.; Borgo, M. D. Self-assembly of trifunctional tripeptides to form neural scaffolds. *J. Mater. Chem. B* **2021**, *9*, 4475−4479.

(14) Immel, J. R.; Chilamari, M.; Bloom, S. Combining flavin photocatalysis with parallel synthesis: a general platform to optimize peptides with non-proteinogenic amino acids. *Chem. Sci.* **2021**, *12*, 10083−10091.
(15) Chalker, J. M.; Gunnoo, S. B.; Boutureira, O.; et al. Methods for converting cysteine to dehydroalanine on peptides and proteins. *Chem. Sci.* **2011**, *2*, 1666−1676.
(16) Seki, M.; Moriya, T.; Kazuo, M. A useful and biomimetic synthesis of *N*-acyl α,β-dehydroalanine from aspartic acid. *Agric. Biol. Chem.* **1984**, *48*, 1251−1255.
(17) Saavedra, C. J.; Hernández, D.; Boto, A. Metal-free, site-selective modification by conversion of "customizable" units into β-substituted dehydroamino acids. *Chem. - Eur. J.* **2018**, *24*, 599−607.
(18) Freedy, A. M.; Matos, M. J.; Boutureira, O.; et al. Chemoselective Installation of Amine Bonds on Proteins through Aza-Michael Ligation. *J. Am. Chem. Soc.* **2017**, *139*, 18365−18375.
(19) Ferreira, P. M. T.; Maia, H. L. S.; Monteiro, L. S.; Sacramento, J. Michael addition of thiols, carbon nucleophiles and amines to dehydroamino acid and dehydropeptide derivatives. *J. Chem. Soc., Perkin Trans. 1.* **2001**, *23*, 3167−3173.
(20) Belokon, Y. N.; Sagyan, A. S.; Djamgaryan, S. M.; Bakhmutov, V. I.; Belikov, V. M. Asymmetric synthesis of β-substituted α-amino acids via a chiral Ni^{II} complex of dehydroalanine. *Tetrahedron.* **1988**, *44*, 5507−5514.
(21) Liu, M.; Sovrovic, M.; Suga, H.; Jongkees, S. A. K. Phosphine addition to dehydroalanine for peptide modification. *Org. Biomol. Chem.* **2022**, *20*, 3081−3085.
(22) Di, L. Strategic approaches to optimizing peptide ADME properties. *AAPS J.* **2015**, *17*, 134−143.
(23) Schlesinger, S.; Schlesinger, M. J. The effect of amino acid analogues on alkaline phosphatase formation in *Escherichia coli* K-12 I. Substitution of triazolealanine for histidine. *J. Biol. Chem.* **1967**, *242*, 3369−3372.
(24) Ferreira, P. M. T.; Maia, H. L. S.; Monteiro, L. S.; Sacramento, J.; Sebastião, J. Synthesis of β-substituted alanines viaMichael addition of nucleophiles to dehydroalanine derivatives. *J. Chem. Soc., Perkin Trans. 1.* **2000**, *19*, 3317−3324.
(25) Riley, L. M.; Mclay, T. N.; Sutherland, A. Synthesis and fluorescent properties of alkynyl- and alkenyl-fused benzotriazole-derived α-amino acids. *J. Org. Chem.* **2023**, *88*, 2453−2463.
(26) Qi, X.; Jambu, S.; Ji, Y.; et al. Late-stage modification of oligopeptides by nickel-catalyzed stereoselective radical addition to dehydroalanine. *Angew. Chem., Int. Ed.* **2022**, *61*, No. e202213315.
(27) Asano, W.; Yamanaka, K.; Ohara, Y.; et al. Fragment-based discovery of novel VE-PTP inhibitors using orthogonal biophysical techniques. *Biochemistry* **2023**, *62*, 2161−2169.
(28) Amarasinghe, K. K. D.; Evidokimov, A. G.; Xu, K.; et al. Design and synthesis of potent, non-peptidic inhibitors of HPTPβ. *Bioorg. Med. Chem. Lett.* **2006**, *16*, 4252−4256.
(29) Lund, I. K.; Andersen, H. S.; Iversen, L. F.; et al. Structure-based design of selective and potent inhibitors of protein tyrosine phosphatase β. *J. Biol. Chem.* **2004**, *279*, 24226−24235.
(30) Bate, N.; Lodge, J.; Brindle, N. P. J. Intrinsic differences in the mechanisms of Tie2 binding to angiopoietins exploited by directed evolution to create an Ang2-selective ligand trap. *J. Biol. Chem.* **2021**, *297*, No. 100888.
(31) Ribatti, D. Chapter 5 Chick embryo chorioallantoic membrane as a useful tool to study angiogenesis. *Int. Rev. Cell. Mol. Biol.* **2008**, *270*, 181−224.
(32) Rodríguez Ugalde, A.; Bloom, S. Beta azole tripeptides: First in-class azole sustained vasodilators. US63/639,361. (U.S. Provisional Patent), 2024.
(33) Kim, J. S.; Chang, J. H.; Yu, H. K.; et al. Inhibition of angiogenesis and angiogenesis-dependent tumor growth by the cryptic kringle fragments of human apolipoprotein(a). *J. Biol. Chem.* **2003**, *278*, 29000−29008.
(34) Li, G.; Nottebaum, A. F.; Brigell, M.; et al. A small molecule inhibitor of VE-PTP activates Tie2 in Schlemm's canal increasing outflow facility and reducing intraocular pressure. *Invest. Ophthalmol. Visual Sci.* **2020**, *61*, No. 12.
(35) Tournaire, R.; Simon, M.; Noble, F. l.; et al. A short synthetic peptide inhibits signal transduction, migration and angiogenesis mediated by Tie2 receptor. *EMBO Rep.* **2004**, *5*, 262−267.
(36) The Day 6 embryo has a weight of 267.5 ± 9.7 mg. See: Hu, N.; Clark, E. B. Hemodynamics of the stage 12 to stage 29 chick embryo. *Circ. Res.* **1989**, *65*, 1665−1670.
(37) Dominguez, M. G.; et al. Vascular endothelial tyrosine phosphatase (VE-PTP)-null mice undergo vasculoneogenesis but die embryonically because of defects in angiogenesis. *Proc. Natl. Acad. Sci. U.S.A.* **2007**, *104*, 3243−3248.
(38) Winderlich, M.; Keller, L.; Cagna, G.; et al. VE-PTP controls blood vessel development by balancing Tie-2 activity. *J. Cell Biol.* **2009**, *185*, 657−671.
(39) Ferrari, R.; Camici, P. G.; Crea, F.; et al. A 'diamond' approach to personalized treatment of angina. *Nat. Rev. Cardiol.* **2018**, *15*, 120−132.
(40) Swaminathan, A.; Balaguru, U. M.; Manjunathan, R.; et al. Live Imaging and Analysis of Vasoactive Properties of Drugs Using an *in-ovo* Chicken Embryo Model: Replacing and Reducing Animal Testing. *Microsc. Microanal.* **2019**, *25*, 961−970.
(41) Gilani, S. H.; Alibhai, Y. Teratogenicity of metals to chick embryos. *J. Toxicol. Environ. Health* **1990**, *30*, 23−31.
(42) Ayala, I.; Perez, G.; Domenech, G.; Castells, M. T.; Valdes, M. Use of the chicken as an experimental animal model in atherosclerosis. *Avian. Poult. Biol. Rev.* **2005**, *16*, 151−159.
(43) Bo, W. J.; Mercuri, M.; Tucker, R.; Bond, G. M. The human carotid atherosclerotic plaque stimulates angiogenesis on the chick chorioallantoic membrane. *Atherosclerosis* **1992**, *94*, 71−78.
(44) Ribatti, D.; et al. Lipoprotein (a) induces angiogenesis on the chick embryo chorioallantoic membrane. *Eur. J. Clin. Invest.* **1998**, *28*, 533−537.
(45) Koide, M.; Harayama, H.; Iio, A.; et al. Major risk factors for atherosclerosis are manifested in experimental Ca-deficiency. *Hypertens. Res.* **1996**, *19*, 35−40.
(46) Rodbard, S.; Katz, L. N.; Bolene, C.; et al. The age factor in hypercholesteremia and atheromatosis in the chick. *Circulation* **1951**, *3*, 867−874.

https://doi.org/10.1021/jacsau.4c00603
JACS Au 2024, 4, 3910−3920